

Slow Relaxation of the Magnetization of an Mn^{III} Single IonRyuta Ishikawa,[†] Ryo Miyamoto,[‡] Hiroyuki Nojiri,[§] Brian K. Breedlove,[†] and Masahiro Yamashita^{*,†,⊥}[†]Department of Chemistry, Graduate School of Science, Tohoku University, 6-3 Aramaki-Aza-Aoba, Aoba-ku, Sendai, Miyagi 980-8578, Japan[⊥]Core Research for Evolutional Science and Technology (CREST), Japan Science and Technology Agency (JST), 4-1-8 Kawaguchi, Saitama 332-0012, Japan[‡]Department of Materials Science and Technology, Faculty of Science and Technology, Hirosaki University, Bunkyo-cho, Hirosaki, Aomori 036-856, Japan[§]Institute for Materials Research, Tohoku University, 2-1-1 Katahira, Aoba-ku, Sendai, Miyagi 980-8577, Japan

Supporting Information

ABSTRACT: A Mn^{III}-salen-type complex with a diamagnetic [Co^{III}(CN)₆]³⁻ moiety, [Mn^{III}(5-TMAM(R)-salmen)(H₂O)Co^{III}(CN)₆·7H₂O·MeCN (**1**; 5-TMAM(R)-salmen = (R)-N,N'-(1-methylethylene)bis(5-trimethylammoniummethylsalicylideneimine)], was prepared. From direct-current magnetic susceptibilities, magnetization, and high-field and multifrequency electronic spin resonance measurements on powdered samples, **1** has a significant uniaxial anisotropy. Frequency-dependent alternating-current susceptibility signals were clearly observed, indicating slow magnetic relaxation. Thus, complex **1** behaves as a single-ion magnet.

New molecular magnetic materials on the nanosize level are needed for future innovation in information technology. One particular interesting class of magnetically bistable molecules are single-molecule magnets (SMMs), which have been shown to exhibit slow magnetic relaxation at low temperatures.¹ The slow magnetic relaxation originates from uniaxial magnetic anisotropy (*D*) and a high-spin (HS) ground state (*S*_T), causing an energy barrier for spin reversal [$\Delta = |D|S_T^2$ or $|D|(S_T^2 - 1/4)$ for integer and half-integer spin systems]. Such molecular nanomagnets show typical quantum tunneling of the magnetization with a long coherence time and can be applied to quantum computing and high-density information storage.² Since the mixed-valence Mn₁₂ cluster was reported as the first SMM, much effort has been devoted to searching for other examples of clusters with 3d and/or 3d–4f metal ions exhibiting SMM behavior.^{1,3} In subsequent studies, the strong spin–orbit coupling involved in the magnetic single ions leading to SMM-like behavior with remarkably high activation energy barriers, which are known as single-ion magnets (SIMs), have been investigated. The first reported SIMs contained 4f ions,⁴ and more recently, SIM behavior has been reported for 5f and 3d ions.^{5,6} The ligand field of 3d metal ions (i.e., magnetic anisotropy of the metal ion) can be controlled via ligand design. Herein we report a new SIM composed of a HS Mn^{III}-salen-type complex, which displays slow relaxation of the magnetization.

Single crystals of [Mn^{III}(5-TMAM(R)-salmen)(H₂O)Co^{III}(CN)₆·7H₂O·MeCN (**1**; 5-TMAM(R)-salmen = (R)-N,N'-(1-methylethylene)bis(5-trimethylammoniummethylsalicy-

lideneimine)] were obtained at the interface between an MeCN solution of [Mn^{III}(5-TMAM(R)-salmen)(H₂O)₂](ClO₄)₃·H₂O and an aqueous solution of K₃[Co^{III}(CN)₆] allowed to diffuse together. From single-crystal X-ray analysis, **1** consists of a neutral Mn^{III}–Co^{III} unit and seven H₂O and one MeCN molecules. The Mn^{III} center has elongated tetragonal geometry with equatorial positions occupied by an N₂O₂ donor set from 5-TMAM(R)-salmen, one apical position occupied by a cyanide N atom of diamagnetic [Co^{III}(CN)₆]³⁻, and the other occupied by an O atom of H₂O. Only one of the six CN groups of the diamagnetic [Co^{III}(CN)₆]³⁻ unit coordinates to the Mn^{III} center (Figure 1).⁷ The 5-TMAM(R)-salmen ligand adopts an envelope

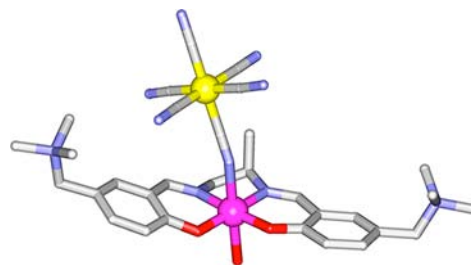


Figure 1. Molecular structure of the [Mn^{III}(5-TMAM(R)-salmen)(H₂O)Co^{III}(CN)₆] unit in **1**. Purple, yellow, blue, red, and gray balls and sticks represent Mn, Co, N, O, and C atoms, respectively. H atoms are omitted for clarity. Selected interatomic distances (Å) and angles (deg) around the Mn^{III} ion: Mn–O_{phenolate} 1.895(av), Mn–N_{imine} 1.993(av), Mn–N_{CN} 2.228(7), Mn–O_{water} 2.317(6), Mn–Co 5.218(6); O_{water}–Mn–N_{cyanide} 175.16(19), Mn–N_{cyanide}–C_{cyanide} 160.5(5).

conformation with a torsion angle of 36.6(8)° involving the N_{imine}–C–C–N_{imine} backbone and an average dihedral angle of 17.64° between phenyl rings in the crystal packing. The axial bond distances are much longer than the equatorial ones because of Jahn–Teller distortion. The neutral Mn^{III}–Co^{III} units self-assemble via a one-dimensional hydrogen-bonding network with O–H···N contacts between the H₂O molecule coordinating on the Mn^{III} ion and the one of uncoordinated CN groups of neighboring Mn^{III}–Co^{III} units. Furthermore, the solvents of

Received: May 29, 2013

Published: July 5, 2013

crystallization form intermolecular hydrogen-bonding networks with the free CN groups on the $\text{Mn}^{\text{III}}\text{--Co}^{\text{III}}$ units.

From measurements of the temperature dependence of the direct-current (dc) magnetic susceptibility data on polycrystalline samples of **1**, the value of $\chi_{\text{M}}T$ was determined to be $3.0 \text{ cm}^3 \text{ K mol}^{-1}$ at 300 K, which corresponds to a single pure HS Mn^{III} ion ($3d^4$, $S = 2$) with $g = 2.0$, and there was no magnetic contribution from the $[\text{Co}^{\text{III}}(\text{CN})_6]^{3-}$ moiety because of the diamagnetic low-spin (LS) Co^{III} ion. The $\chi_{\text{M}}T$ value remained constant at $\sim 70 \text{ K}$ and then abruptly decreased at lower temperatures (Figure 2). This behavior suggests that there is

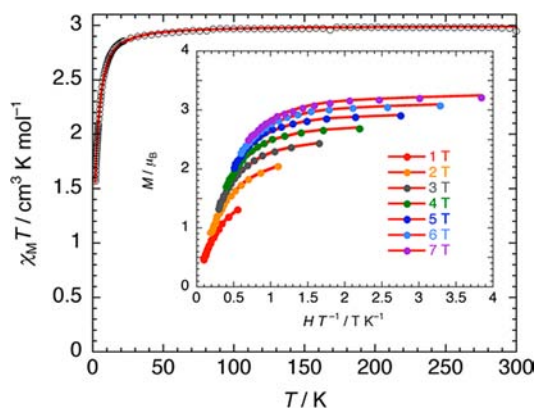


Figure 2. Temperature dependence of $\chi_{\text{M}}T$ for **1** at 1000 Oe. Inset: Field dependence of magnetization curves for **1**, collected from 1.8 to 10 K. The red solid lines represent best-fit curves. The fitting model is described in the text.⁸

appreciable zero-field splitting (ZFS), causing an $S_{\text{Mn}} = 2$ ground state for the Mn^{III} ion, which is typical for other mononuclear HS Mn^{III} derivatives.⁸ Indeed, variable-field magnetization data for **1** at lower temperatures could not be superimposed, showing that there is strong magnetic anisotropy of ZFS of the HS Mn^{III} single ion (inset of Figure 2). The magnetic behavior was fit with an isolated $S_{\text{Mn}} = 2$ ground state with an axial ZFS term D_{Mn} of -3.3 cm^{-1} , a mean-field approximation (MFA) zJ' of -0.07 cm^{-1} , and g_{Mn} of 2.0.⁸

High-field and multifrequency (HF/MF) electronic spin resonance (ESR) measurements on polycrystalline samples of **1** at different temperatures were used to confirm directly the presence of a magnetic anisotropic energy gap between each M_S

level (Figure S1 in the Supporting Information, SI). In low-frequency fields, the signal intensity increased with a decrease in the temperature, which clearly indicates that $D_{\text{Mn}} < 0$,⁹ as required for SIMs. Plots of the frequency (ν) versus resonance field (H) from the HF/MF-ESR spectra are shown in Figure S1 in the SI. Extrapolation of the frequency dependence of the signals of the lowest field to $H = 0$ can be used to estimate the magnetic anisotropy gap because these transitions correspond to the allowed transition $M_S = -2 \leftrightarrow -1$ ($\Delta M_S = 1$). The gap was estimated to be 300 GHz ($=10 \text{ cm}^{-1}$; Figure S2 in the SI), and if $E = 0$, it is equivalent to $-3D_{\text{Mn}}$.¹⁰ Thus, D_{Mn} was estimated to be -3.3 cm^{-1} (Figure S3 in the SI), which is consistent with SQUID magnetic studies (vide supra).

From the low-temperature alternating-current (ac) susceptibility data, **1** exhibits slow magnetic relaxation phenomena in the frequency range of 1–1500 Hz in a zero dc field, where in-phase (χ_{M}') and out-of-phase (χ_{M}'') components of the ac susceptibility of **1** show strong frequency dependence below 3.0 K (right side of Figure 3). This phenomenon is clearly related to the magnetic anisotropy of the HS Mn^{III} ion of **1**. Various dc fields below 4500 Oe were applied to determine if the magnetic relaxation is suppressed in dc fields as expected in the presence of fast zero-field quantum-tunneling relaxation of the magnetization. Although there was a slight effect, the χ_{M}' signals for **1**, which increased with a decrease in the temperature, barely showed any tailing, and the expected maximum value due to blocking could not be observed down to 1.8 K even in an applied dc field of 4500 Oe, as indicated by the divergence of the χ_{M}'' signals (left side of Figure 3).

Nevertheless, the values of Δ ($=|D_{\text{Mn}}|S_{\text{Mn}}^2$) from a negative D_{Mn} acting on S_{Mn} for **1** can be estimated from $\chi_{\text{M}}''/\chi_{\text{M}}'$ versus $1/T$ plots with a semilogarithmic scale at the given frequencies of the ac susceptibility data by using the following equation derived from the Kramers–Kronig equation:¹¹

$$\log\left(\frac{\chi_{\text{M}}''}{\chi_{\text{M}}'}\right) = \log(\omega\tau_0) + \frac{\Delta}{k_{\text{B}}T}$$

where ω ($=2\pi\nu$) is the oscillating frequency of the ac field, τ_0 is a preexponential factor of the Arrhenius law $\tau = \tau_0 \exp(\Delta/k_{\text{B}}T)$, k_{B} is Boltzmann's constant, and T is the temperature.

By fitting the data, the effective Δ (Δ_{eff}) was determined to be ≈ 9.3 and $\approx 11.5 \text{ cm}^{-1}$ with $\tau_0 = \approx 8.0 \times 10^{-8}$ and $\approx 2.9 \times 10^{-7} \text{ s}$ in a zero dc field and an applied dc field of 4500 Oe, respectively. The τ_0 values fall within the range typically observed for SIMs

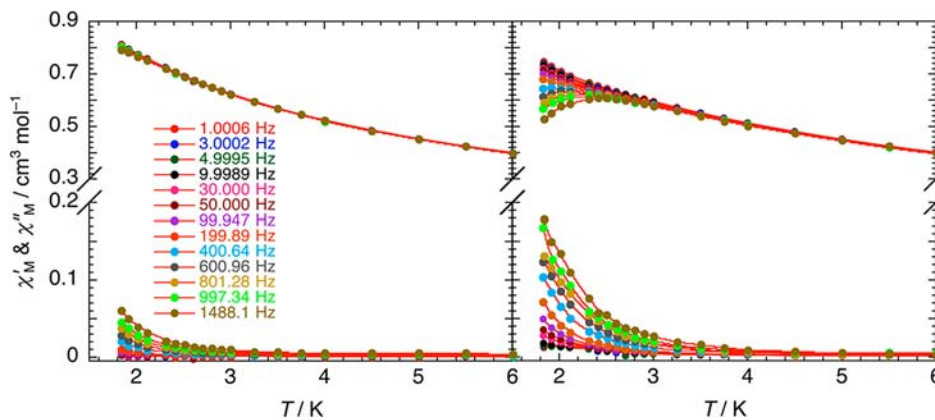


Figure 3. Temperature dependence of the ac susceptibilities (χ_{M}' and χ_{M}'') of **1** in the frequency range of 1–1500 Hz in an oscillating ac magnetic field of 5 Oe in a zero dc field (left) and an applied 4500 Oe dc field (right). The red solid lines serve as guides to the eye.

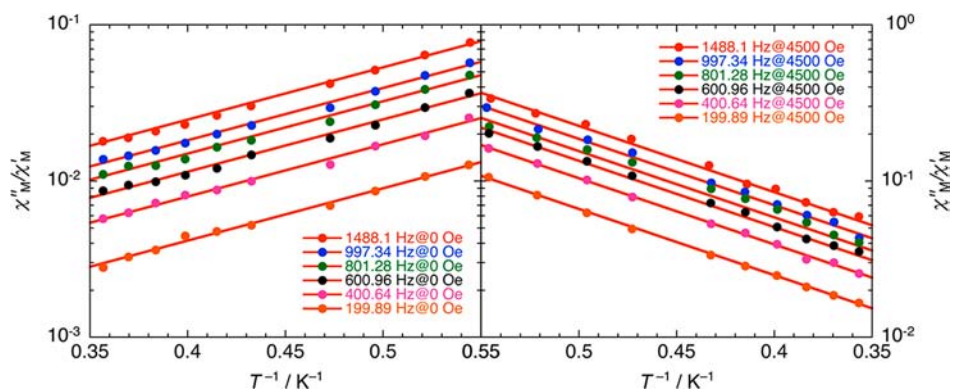


Figure 4. χ''/χ' versus $1/T$ plot for **1** at different frequencies with a semilogarithmic scale. The red solid lines were fitted as described in the text.

and SMMs (Figures 4 and S4 in the SI). Therefore, **1** is an SIM rather than a three-dimensionally ordered magnet.

In summary, SIM features of a new tricationic Mn^{III}-salen-type complex with diamagnetic [Co^{III}(CN)₆]³⁻ moieties were determined. On the basis of dc magnetic susceptibility and magnetization studies, **1** has significant uniaxial anisotropy for an isolated $S_{Mn} = 2$ with $D_{Mn} = -3.3$ cm⁻¹ and $g_{Mn} = 2.0$, which was supported by HF/MF-ESR studies on powdered samples. Consequently, the observed uniaxial magnetic anisotropy leads to slow magnetic relaxation, as evidenced by frequency-dependent ac magnetic susceptibilities.

■ ASSOCIATED CONTENT

Supporting Information

X-ray crystallographic data in CIF format, experimental section, physical measurements, crystallographic data, and data of HF/MF-ESR spectral details. This material is available free of charge via the Internet at <http://pubs.acs.org>.

■ AUTHOR INFORMATION

Corresponding Author

*E-mail: yamasita@agnus.chem.tohoku.ac.jp. Tel: +81-22-795-6548. Fax: +81-22-795-6548.

Author Contributions

All authors discussed the results and commented on the manuscript.

Notes

The authors declare no competing financial interest.

■ ACKNOWLEDGMENTS

This work was financially supported by a Grant-in-Aid for Scientific Research (S) (Grant No. 20225003) from the Ministry of Education, Culture, Sports, Science, and Technology, Japan.

■ REFERENCES

- (1) Gatteschi, D.; Sessoli, R.; Villain, J. *Molecular Nanomagnets*; Oxford University Press: Oxford, U.K., 2006.
- (2) (a) Friedman, J. R.; Sarachik, M. P.; Tejada, J.; Ziolo, R. *Phys. Rev. Lett.* **1996**, *76*, 3830. (b) Bogani, L.; Wernsdorfer, W. *Nat. Mater.* **2008**, *7*, 179.
- (3) (a) Osa, S.; Kido, T.; Matsumoto, N.; Re, N.; Pochaba, A.; Mrozinski, J. *J. Am. Chem. Soc.* **2004**, *126*, 420. (b) Zaleski, F. C. M.; Depperman, E. C.; Kampf, J. W.; Lirk, M. L.; Pecoraro, V. L. *Angew. Chem., Int. Ed.* **2004**, *43*, 3912. (c) Mishra, A.; Wernsdorfer, W.; Abboud, K. A.; Christou, G. *J. Am. Chem. Soc.* **2004**, *126*, 15648.
- (4) (a) Jiang, S.-D.; Wang, B.-W.; Sun, H.-L.; Wang, Z.-M.; Gao, S. *J. Am. Chem. Soc.* **2011**, *133*, 4730. (b) Sorace, L.; Benelli, C.; Gatteschi, D. *Chem. Soc. Rev.* **2011**, *40*, 3092. (c) Chilton, N. F.; Langley, S. K.

Moubaraki, B.; Soncini, A.; Batten, S. R.; Murray, K. S. *Chem. Sci.* **2013**, *4*, 1719.

- (5) (a) Rinehart, J. D.; Long, J. R. *J. Am. Chem. Soc.* **2009**, *131*, 12558. (b) Rinehart, J. D.; Meihaus, K. R.; Long, J. R. *J. Am. Chem. Soc.* **2010**, *132*, 7572. (c) Magnani, N.; Apostolidis, C.; Morgenstern, A.; Colineau, E.; Griveau, J. C.; Bolvin, H.; Walter, O.; Caciuffo, R. *Angew. Chem., Int. Ed.* **2011**, *50*, 1696. (d) Antunes, M. A.; Pereira, L. C. J.; Santos, I. C.; Mazzanti, M.; Marçalo, J.; Almeida, M. *Inorg. Chem.* **2011**, *50*, 9915. (e) Coutinho, J. T.; Antunes, M. A.; Pereira, L. C. J.; Bolvin, H.; Marçalo, J.; Mazzanti, M.; Almeida, M. *Dalton Trans.* **2012**, *41*, 13568. (f) Moro, F.; Mills, D. P.; Liddle, S. T.; van Slageren, J. *Angew. Chem., Int. Ed.* **2013**, *52*, 3430.

- (6) (a) Freedman, D. E.; Harman, W. H.; Harris, T. D.; Long, G. J.; Chang, C. J.; Long, J. R. *J. Am. Chem. Soc.* **2010**, *132*, 1224. (b) Harman, W. H.; Harris, T. D.; Freedman, D. E.; Fong, H.; Chang, A.; Rinehart, J. D.; Ozarowski, A.; Sougrati, M. T.; Grandjean, F.; Long, G. J.; Long, J. R.; Chang, C. J. *J. Am. Chem. Soc.* **2010**, *132*, 18115. (c) Weismann, D.; Sun, Y.; Lan, Y.; Wolmershäuser, G.; Powell, A. K.; Sitzmann, H. *Chem.—Eur. J.* **2011**, *17*, 4700. (d) Lin, P.-H.; Smythe, N. C.; Gorelsky, S. I.; Maguire, S.; Henson, N. J.; Korobkov, I.; Scott, B. L.; Gordon, J. C.; Baker, R. T.; Murugesu, M. *J. Am. Chem. Soc.* **2011**, *133*, 15806. (a) Zadrozny, J. M.; Long, J. R. *J. Am. Chem. Soc.* **2011**, *133*, 20732. (b) Jurca, T.; Farghal, A.; Lin, P.-H.; Korobkov, I.; Murugesu, M.; Richardson, D. S. *J. Am. Chem. Soc.* **2011**, *133*, 15814. (c) Zadrozny, J. M.; Liu, J.; Piro, N. A.; Chang, C. J.; Hill, S.; Long, J. R. *Chem. Commun.* **2012**, *48*, 3927. (d) Vallejo, J.; Castro, I.; Ruiz-García, R.; Cano, J.; Julve, M.; Lloret, F.; De Munno, G.; Wernsdorfer, W.; Pardo, E. *J. Am. Chem. Soc.* **2012**, *134*, 15704. (e) Mossin, S.; Tran, B. L.; Adhikari, D.; Pink, M.; Heinemann, F. W.; Sutter, J.; Szilagy, R. K.; Meyer, K.; Mindiola, D. J. *J. Am. Chem. Soc.* **2012**, *134*, 13651.

(7) Miyasaka, H.; Saitoh, A.; Abe, S. *Coord. Chem. Rev.* **2007**, *251*, 2622.

(8) The spin Hamiltonian was defined by the following expression:

$$\mathcal{H} = \mathcal{H}_{\text{ZFS}} + \mathcal{H}_{\text{MFA}} + \mathcal{H}_{\text{Zeeman}}$$

where $\mathcal{H}_{\text{ZFS}} = D_{\text{Mn}}[S_z^2 - (S(S+1))/3]$, $\mathcal{H}_{\text{MFA}} = -J'S_{\text{Mn}}\langle S_{\text{Mn}} \rangle$, and $\mathcal{H}_{\text{Zeeman}} = g_{\text{Mn}}\mu_B S_{\text{Mn}}H$. (a) Kennedy, B. J.; Murray, K. S. *Inorg. Chem.* **1985**, *24*, 1552. (b) Baba, H.; Nakano, M. *Polyhedron* **2009**, *28*, 2087.

(9) Gatteschi, D.; Barra, A. L.; Caneschi, A.; Cornia, A.; Sessoli, R.; Sorace, L. *Coord. Chem. Rev.* **2006**, *250*, 1514.

(10) If $E \neq 0$ (E is the rhombic component of the ZFS), the energy gap is $-3(D + |E| + |E|^2/D)$.

(11) Bartolomé, J.; Filoti, G.; Kuncser, V.; Schinteie, G.; Mereacre, V.; Anson, C. E.; Powell, A. K.; Prodius, D.; Turta, C. *Phys. Rev. B* **2009**, *80*, 014430.